Springer
Acta Mechanica Sinica

• RESEARCH PAPER •

Acta Mech. Sin., Vol. 39, 421602 (2023)
https://doi.org/10.1007/s10409-022-21602-x

A non-probabilistic convex polyhedron model for reliability analysis of structures with multiple failure modes and correlated uncertainties based on limited data

Zhiping Qiu[1*], Haijun Tang[2], and Bo Zhu[1]

[1] Institute of Solid Mechanics, Beihang University, Beijing 100191, China;
[2] Chengdu Aircraft Design & Research Institute, Aviation Industry Corporation of China, Chengdu 610091, China

Received September 15, 2022; accepted October 8, 2022; published online November 24, 2022

This paper proposes a novel non-probabilistic reliability model called the convex polyhedron reliability model, focusing on structural reliability assessment under uncertain conditions. Unlike existing probabilistic and non-probabilistic interval models, the convex polyhedron model considers the situation where a multi-dimensional convex polyhedron describes the uncertain variable space. Compared with the interval model, the convex polyhedron model is more compact and reflects the correlation between uncertain variables based on limited information. The area/volume ratio is introduced to be referred to as the reliability index in the proposed framework. Then the case of the nonlinear limit state function is discussed and addressed by the most likely failure point-based linearization method and the piecewise linearization method. Furthermore, this paper investigates an effective approach to dealing with the structural system reliability analysis problem with multiple failure modes based on the proposed non-probabilistic convex polyhedron reliability model. Finally, three examples are provided to verify the effectiveness and applicability of the proposed method. Through comparison with the existing reliability models, the results show that the reliability evaluated by the probabilistic reliability model and non-probabilistic reliability model are compatible.

Non-probabilistic uncertainties, Structural reliability analysis, Convex polyhedron, Multiple failure modes

Citation: Z. Qiu, H. Tang, and B. Zhu, A non-probabilistic convex polyhedron model for reliability analysis of structures with multiple failure modes and correlated uncertainties based on limited data, Acta Mech. Sin. **39**, 421602 (2023), https://doi.org/10.1007/s10409-022-21602-x

1. Introduction

The widespread uncertainty in the real world has become a consensus, especially in aerospace, electrical and electronic, ship, automobile, and other engineering fields. Uncertainty factors include manufacturing tolerance, random material parameters, assembly error, load, etc [1-4]. Ignoring the existence of uncertainty will lead to a series of security problems. Thus, uncertainty research is unavoidable. There are currently three main ways to deal with engineering uncertainty—the probabilistic model, the fuzzy set model, and the non-probabilistic set model [5].

The probabilistic model has been widely used to handle the uncertainty in the real structure, which is the most commonly used method to solve the reliability problem, and has formed a series of mature reliability analysis techniques [6-10]. For some types of probabilistic distributions, such as Gaussian distribution, random variables are defined within the infinity space, but in actually, the variables are generally studied with truncated distribution. The truncated probabilistic reliability theory is thus established for such truncated probabilistic distribution [11]. An improved first-order reliability method (FORM) is proposed by Du et al. [12] to evaluate the reliability of structures with truncated random variables. Zhang et al. [13] proposed a method for reliability and sensitivity analysis of structural systems using the truncated reliability method. Sufficient information of uncertainties is necessary to construct an accurate and reasonable probabilistic density distribution. However, it is difficult to obtain enough samples of uncertainties in prac-

*Corresponding author. E-mail address: zpqiu@buaa.edu.cn (Zhiping Qiu)
Executive Editor: Jianxiang Wang

tice because the related experiments are time-consuming and expensive to be carried out for engineering structures. It was stated in Refs. [14,15] that even minor errors in probabilistic data might lead to significant errors in the estimated failure probability. Hence, when the data is limited, the probabilistic model may no longer be suitable for reliability evaluation. Regarding the fuzzy set model [16-20], the acquisition of membership functions depends more on users' subjective experience than objective experimental data. As a result, different fuzzy membership functions can be defined with the same group of samples, and it is not easy to evaluate the quality of these membership functions, bringing a challenge to the reasonable evaluation of reliability.

In recent decades, many scholars have reached an agreement that the non-probabilistic convex set models, mainly including the interval model, the ellipsoid model, and the convex polyhedron model, are more suitable and reasonable when the information of uncertainties is lacking. Some non-probabilistic methods have been developed for reliability analysis. Ben-Haim et al. [14,21] and Elishakoff et al. [22] proposed and developed the convex model to describe the data in default of uncertainty information, and then the concept of non-probabilistic reliability based on convex set theory is proposed for the first time by Ben-Haim [23]. Qiu et al. [24] pointed out that there might be errors in Ben-Haim's robust reliability theory, and the correctional structural reliability was proposed using the stress-strength interference. Further, the concept of non-probabilistic reliability was extensively discussed on more areas, such as the structural flutter, fracture mechanics, and structural vibration [25-27].

In terms of the interval model, based on the stress-intensity interference model, Wang et al. [28] proposed an efficient scheme to calculate the volume ratio of the safety region to the total region constructed by the interval variables as an index of structural reliability. Guo et al. [29-31] introduced the traditional first-order reliability method into the interval convex model, according to which the interval reliability could be evaluated in the case of the nonlinear limit state function, and presented an analytical calculation method for the interval reliability. As another kind of non-probabilistic convex set model, the ellipsoid model describes the uncertain domain as a multi-dimensional ellipsoid, in which the uncertain variables are assumed to be correlated. Jiang et al. [32,33] proposed a correlation analysis technique for the multi-dimensional ellipsoid model and presented a non-probabilistic reliability analysis model for ellipsoid uncertainties. Cao and Duan [34] constructed a reliability index for ellipsoid models based on the minimum distance in the standard variable space. Besides, some other studies [35-37] on ellipsoid convex models have also been performed by researchers. In general, the interval model can only deal with independence problems, while the ellipsoid model can only address the problems of correlation. Jiang et al. [38,39] proposed a new convex model called multi-dimensional parallelepiped (MP) model, which is a more general convex model that can consider independent and dependent variables in a unified framework. Then, integrating multi-dimensional ellipsoid models and MP models, a unified construction framework for these convex models was offered through the correlation analysis approach, in which an evaluation criterion for convex modeling methods was also presented [40]. Besides, considering time-variant and spatially varying uncertainties, studies on interval process [27], convex model process [41] and bounded field models [42] were successively carried out, significantly promoting the development of convex model-based uncertainty analysis and reliability evaluation.

Nowadays, the convex polyhedron is widely used in computer graphics, image processing, and pattern recognition. However, the majority of current research focuses on ellipsoidal and interval models, and the application of convex polyhedrons in structural reliability is rarely studied. In terms of uncertainty quantification, the interval model cannot consider the correlation between uncertain variables, and the ellipsoid convex model can only consider the variables with correlation. Although the multi-dimensional parallel piped model can consider both correlated and uncorrelated variables, but its form is simpler than that of the convex polyhedron model, so the model will lose correlation in the construction of complex correlation variables. By comparison, the convex polyhedron can better fit the sample data and construct a more compact uncertainty region which can handle both correlation and independent variables. At the same time, the correlation between variables is preserved to the greatest extent. As shown in Fig. 1, the convex polyhedron model is able to represent the spatial distribution characteristic of the current data more accurately.

On account of the above advantages, to investigate the potential of convex polyhedron in reliability analysis, in contrast to existing studies, this paper describes uncertainties by convex polyhedron models, based on which the corresponding reliability analysis approach is studied.

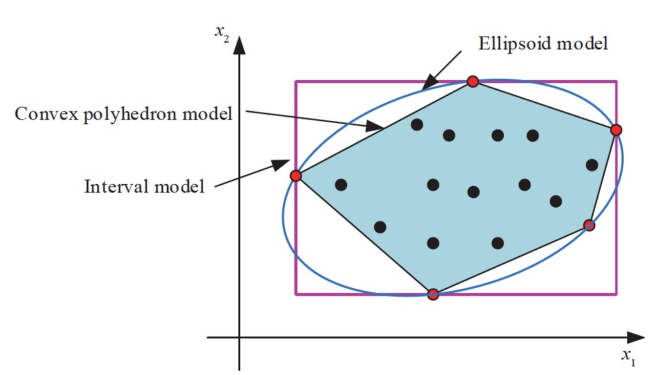

Figure 1 Three different models to envelop the experimental samples.

The novelty of this work is stated as follows. First, we introduce the convex polyhedron model to achieve a compact description of non-probabilistic uncertainties with correlation considered. Then, using the definition of convex polyhedron, it is found that the failure region can also be modelled by a convex polyhedron under linear cases, resulting in convenient acquirement of its area (or volume). Accordingly, a novel non-probabilistic convex polyhedron reliability model is proposed based on the area (or volume) ratio index. Meanwhile, the most likely failure point-based and piecewise linearization methods are introduced to construct the convex polyhedron model for the failure region under nonlinear cases. Further, situation of multiple failure modes is discussed and convex polyhedron model for structural comprehensive failure (or safety) region is derived.

The remainder of this paper is organized as follows. The traditional probabilistic reliability analysis model and measurement of structural interval reliability are reviewed in Sects. 2 and 3, respectively. In Sect. 4, the index of structural convex-polyhedron reliability is studied. Structural system reliability analysis for convex polyhedron model problems is studied in Sect. 5. Section 6 demonstrates the efficiency and applicability of the proposed method by a numerical example and two engineering examples. Finally, some conclusions are presented in Sect. 7.

2. Conventional probabilistic reliability analysis model

The probabilistic reliability model regards uncertain parameters as random variables, because of which the following limit state function is a random function as well.

$$M = g(\mathbf{x}) = g(x_1, x_2, \cdots, x_n), \tag{1}$$

where $x_1, x_2, \cdots, x_n$ represent random variables. M is the limit state function value. $g(\mathbf{x}) = 0$ represents the failure surface (or the limit state surface), dividing the variable space into the failure region and the safety region. Moreover, $\Omega_\mathrm{s} = \{\mathbf{x} : g(\mathbf{x}) > 0\}$ denotes the safety region, while $\Omega_\mathrm{f} = \{\mathbf{x} : g(\mathbf{x}) < 0\}$ denotes the failure region. Measured by random probability, probabilistic reliability is theoretically defined as

$$\begin{aligned} P_\mathrm{s} &= 1 - P_\mathrm{f} \\ &= 1 - \int \cdots \int_{\Omega_\mathrm{f}} f_\mathrm{joint}(x_1, x_2, \cdots, x_n) \mathrm{d}x_1 \mathrm{d}x_2 \cdots \mathrm{d}x_n, \end{aligned} \tag{2}$$

or

$$P_\mathrm{s} = \int \cdots \int_{\Omega_\mathrm{s}} f_\mathrm{joint}(x_1, x_2, \cdots, x_n) \mathrm{d}x_1 \mathrm{d}x_2 \cdots \mathrm{d}x_n, \tag{3}$$

where P_s and P_f stand for the safety probability and failure probability, respectively. $f_\mathrm{joint}(x_1, x_2, \cdots, x_n)$ is the joint probability density function of $\mathbf{x}$. The integral domains in Eqs. (2) and (3) are the failure region Ω_s and safety region Ω_f, respectively.

In practical conditions, the value range of random variables will not be set to infinity, and the variable space is usually truncated to a finite region, such as

$$\underline{x}_i \le x_i \le \overline{x}_i, \ i = 1, 2, \cdots, n, \tag{4}$$

where $\underline{x}_i$ and $\overline{x}_i$ are the lower bound and upper bound of the i-th truncated uncertain parameter.

Since the given variable vector $\mathbf{x}$ has been truncated, the joint probability density function in Eq. (3) should also be a truncated joint probability density function as follows:

$$f^*_\mathrm{joint}(\mathbf{x}) = \begin{cases} f_\mathrm{joint}(\mathbf{x}) / J, & \underline{x}_i \le x_i \le \overline{x}_i, \ i = 1, 2, \cdots, n, \\ 0, & \text{others}, \end{cases} \tag{5}$$

where

$$\begin{aligned} &J = \int_\Omega f_\mathrm{joint}(\mathbf{x}) \mathrm{d}\mathbf{x}, \\ &\Omega = \{x_i : -1 \le x_i \le 1 \, (i = 1, 2, \cdots, n)\}. \end{aligned} \tag{6}$$

Hence, substituting Eq. (5) into Eq. (3) yields the following truncated reliability:

$$P_{\mathrm{s,t}} = \int_{\Omega_\mathrm{s}} f^*_\mathrm{joint}(\delta_x) \mathrm{d}\mathbf{x} = \frac{1}{J} \int_{\Omega_\mathrm{s}} f_\mathrm{joint}(\delta_x) \mathrm{d}\mathbf{x}, \tag{7}$$

where Ω_s is the safety region and the Monte Carlo method can be used to estimate Eq. (7).

3. Non-probabilistic interval reliability analysis model

When the amount of samples is not enough to determine the probabilistic density function of the variable, the bounded interval model is utilized to describe the uncertainty with the upper and lower bounds. Although the range of random variables is also bounded in truncated probabilistic models stated in Sect. 2, these variables are of specific probabilistic density functions in the truncated region. Besides, one of the key differences between the interval model and probabilistic model is that the former only pays attention to the upper and lower bounds of uncertainties. At the same time, the latter focuses on the probability distribution information, such as the mean value, variance, or probabilistic density function. Hence, the interval model is also known as the non-probabilistic interval model.

In the framework of non-probabilistic interval models, the uncertain parameters in structures are assumed to be interval variables, i.e., $\mathbf{x} \in \mathbf{x}^\mathrm{I} = [\underline{\mathbf{x}}, \overline{\mathbf{x}}]$. $\overline{\mathbf{x}} = (\overline{x}_1, \overline{x}_2, \cdots, \overline{x}_n)^\mathrm{T}$ and $\underline{\mathbf{x}} = (\underline{x}_1, \underline{x}_2, \cdots, \underline{x}_n)^\mathrm{T}$ are the upper bound and the lower bound vectors of the parameter vector $\mathbf{x}$, respectively. The nominal value vector $\mathbf{x}^\mathrm{c}$ and radius vector $\mathbf{x}^\mathrm{r}$ of interval variables are defined as

$$\mathbf{x}^{\mathrm{c}} = \frac{1}{2}(\overline{\mathbf{x}} + \underline{\mathbf{x}}), \quad \mathbf{x}^{\mathrm{r}} = \frac{1}{2}(\overline{\mathbf{x}} - \underline{\mathbf{x}}). \tag{8}$$

In one-dimensional, two-dimensional (2-D) and three-dimensional (3-D) cases, the variable space of the uncertain vector $\mathbf{x}$ is an interval, a rectangle and a box, respectively. Without loss of generality, in n-dimensional cases, uncertain vecter $\mathbf{x}$ locates in a n-dimensional hyper-rectangle.

In terms of reliability analysis problems, as stated in Sect. 2, the failure surface divides the variable space into the failure region and the safety region. As shown in Fig. 2, when the uncertain parameters are described by non-probabilistic interval models, the 2-D variable space of $\mathbf{x} = (x_1, x_2)^{\mathrm{T}}$ is a rectangle, and $g(\mathbf{x}) = 0$ is assumed to be linear. There are three conditions of the relationship between the failure plane and variable space.

Condition (1) is that the failure plane does not intersect the variable space, which means that the whole space is a safety region. Condition (2) is that the failure plane intersects the variable space at a single point, representing a critical state. Condition (3) is that the failure plane intersects the variable space and divides it into the safety region and failure region.

When conditions (1) and (2) occur, it is considered that the structure is safe. When it comes to condition (3), it is necessary

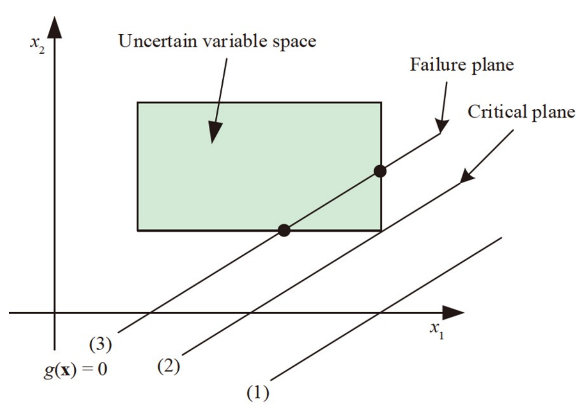

Figure 2 Different relationships between the failure plane and uncertain variable space.

to evaluate the non-probabilistic reliability. Figure 3 shows the safety region and failure region in 2-D and 3-D cases, respectively. Referring to Ref. [28], the non-probabilistic reliability index is defined as the ratio of the area or volume of safety region to that of the whole variable space, namely

$$P_{\mathrm{s}}^{\mathrm{I}} = \frac{V_{\mathrm{safe}}}{V_{\mathrm{total}}}, \tag{9}$$

where $P_{\mathrm{s}}^{\mathrm{I}}$ is the safety index in the non-probabilistic interval reliability model. V_{safe} and V_{total} are the measurement of the safety region and the whole variable space, respectively. Similarly, the failure index is defined as the ratio of area or volume of failure region to that of the whole variable space, namely

$$P_{\mathrm{f}}^{\mathrm{I}} = \frac{V_{\mathrm{failure}}}{V_{\mathrm{total}}}. \tag{10}$$

The safety index and failure index hold

$$P_{\mathrm{s}}^{\mathrm{I}} + P_{\mathrm{f}}^{\mathrm{I}} = 1. \tag{11}$$

As shown in Fig. 3, owing to the simplicity of the non-probabilistic interval model, the safety region and failure region are concise and regular in geometry, so the non-probabilistic interval reliability indices can be more easily obtained by some basic mathematical operations rather than complex probability analysis in the probabilistic reliability analysis model.

However, it is undeniable that the reliability assessed by probabilistic models has a stronger statistical significance, while the non-probabilistic interval model is an optional reliability analysis model in the cases of limited data. The applicable conditions of the above two categories of reliability analysis models are different based on the data size.

4. Convex polyhedron reliability analysis model

This section provides a novel non-probabilistic reliability analysis model based on uncertainties modeled by convex polyhedrons, which is a generalization of the interval model after considering the parameter correlation. If we adopt the

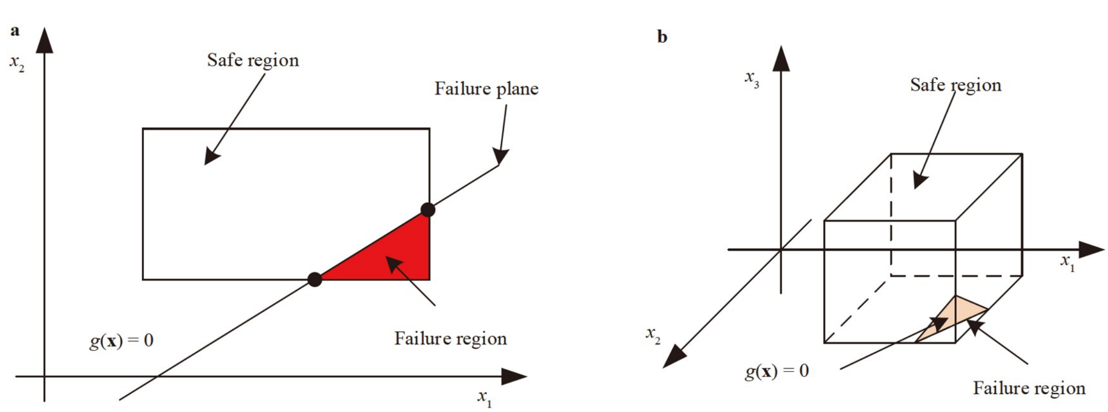

Figure 3 Safety and failure region in the interval reliability model. **a** 2-D reliability; **b** 3-D reliability.

convex polyhedron model to describe the uncertainties, the variable space of uncertain variables will be a convex polyhedron rather than a hype-rectangle in the interval model [43].

4.1 Construction of the convex polyhedron

Suppose that the uncertain variables in limit state functions are described as convex polyhedrons, in which the variable vector can be expressed via the combination of several vertex vectors as follows [44]:

$$\mathbf{x} = \sum_{i=1}^{N} \alpha_i \mathbf{x}_i^{\mathrm{v}}, \tag{12}$$

where N is the total number of vertex vectors of the convex polyhedron. $\mathbf{x} = (x_1, x_2, \cdots, x_n)^{\mathrm{T}}$ is the uncertain variable vector. $\mathbf{x}_i^{\mathrm{v}} = \left(x_{i1}^{\mathrm{v}}, x_{i2}^{\mathrm{v}}, \cdots, x_{in}^{\mathrm{v}}\right)^{\mathrm{T}}$ is the vertex vector of the convex polyhedrons. $\boldsymbol{\alpha} = (\alpha_1, \alpha_2, \cdots, \alpha_N)^{\mathrm{T}}$ is weight vector for each vertex and holds

$$\sum_{i=1}^{N} \alpha_i = 1, \ \ \alpha_i \geq 0. \tag{13}$$

All the vectors satisfying Eq. (12) form a convex polyhedron. That is to say, once the vertex vectors are determined, a convex polyhedron can be constructed.

For simplicity, there is another way called closed semi-space representation to describe the convex polyhedron, namely

$$\Omega_{\mathrm{c}} = \{\mathbf{x} \in \mathbf{R}^n | \mathbf{A}\mathbf{x} \leq \mathbf{b}\}, \tag{14}$$

where $\mathbf{A}$ is a matrix, and $\mathbf{b}$ is a vector. Every component of the linear inequalities represents a facet of the convex polyhedron and reflects the correlation between the variables. It is worth mentioning that the two expressions (i.e., the vertex representation Eq. (12) and closed semi-space representation Eq. (14)) are equivalent, which can be converted to each other [44].

As for 2-D cases, Fig. 1 shows the relationship between the interval model and the convex polyhedron model. For given sample points, the interval model only considers the extreme value of each variable using a rectangle to envelop all sample points. By contrast, the convex polyhedron model utilizes a smaller convex hull to envelope all sample points. As can be seen from Fig. 4, there are countless convex polyhedrons that can encircle the given sample points. However, the minimum convex polyhedron (MCP) is indeed unique, of which the vertex points are selected from the existing sample points. Hence, as long as the sample points of uncertain variables are given, a unique MCP can be determined. In this work, the quickhull algorithm (QA) [45] is introduced to construct the convex polyhedron, which is an effective approach to selecting the vertices of MCP from the given samples.

Notably, the convex polyhedron model studied in this work is based on the minimum convex model that can envelop all the sample points so that it can describe the experimental sample points most compactly and reflect the correlation between uncertainty parameters.

4.2 Convex polyhedron reliability analysis considering the linear limit state function

Since the convex polyhedron model belongs to the non-probabilistic model, therefore, the area ratio and volume ratio stated in Sect. 3 are employed as the reliability measurement indices in the proposed convex polyhedron reliability analysis model in this section.

In order to concisely describe the framework of the proposed convex polyhedron model, the case of linear limit state functions is firstly considered, which is the most fundamental case. The linear limit state function of the structure can be written as follows:

$$M = g(\mathbf{x}) = a_0 + \sum_{i=1}^{n} a_i x_i = a_0 + \mathbf{a}^{\mathrm{T}}\mathbf{x}, \tag{15}$$

where $\mathbf{a} = (a_1, a_2, \cdots, a_n)^{\mathrm{T}}$.

Suppose that the variable space has been described as a convex polyhedron in the form of Eq. (14). Then the safety region Ω_{s} and failure region Ω_{f} are also convex polyhedrons expressed as follows:

$$\begin{aligned} \Omega_{\mathrm{s}} &= \left\{ \mathbf{x} \in \mathbf{R}^n \left| \begin{bmatrix} \mathbf{A} \\ -\mathbf{a}^{\mathrm{T}} \end{bmatrix} \mathbf{x} \leq \begin{bmatrix} \mathbf{b} \\ \mathbf{a}_0 \end{bmatrix} \right. \right\}, \\ \Omega_{\mathrm{f}} &= \left\{ \mathbf{x} \in \mathbf{R}^n \left| \begin{bmatrix} \mathbf{A} \\ \mathbf{a}^{\mathrm{T}} \end{bmatrix} \mathbf{x} \leq \begin{bmatrix} \mathbf{b} \\ -\mathbf{a}_0 \end{bmatrix} \right. \right\}. \end{aligned} \tag{16}$$

Next, taking the 2-D case as an example, the convex polyhedron reliability analysis model is illustrated in conjunction with Fig. 5. It can be seen that the limit state plane

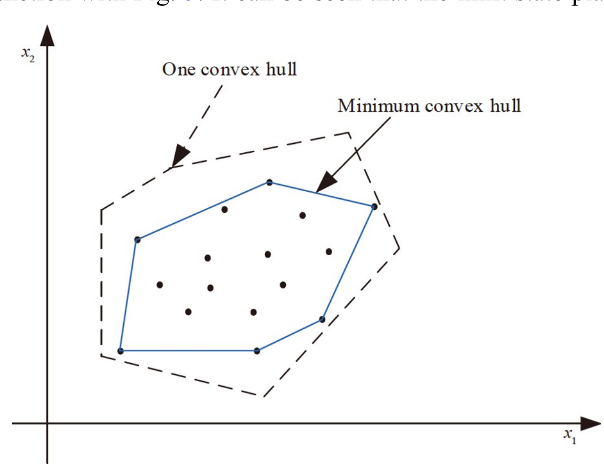

Figure 4 The minimum convex hull to encircle the given samples.

divides the original variable space into two convex polyhedrons, namely the safety region and failure region expressed in Eq. (16).

In the same way as derived in Eqs. (9) and (10), the convex polyhedron reliability indices are given as follows:

$$P_s^c = \frac{V_{safe}}{V_{total}}, \tag{17}$$

$$P_f^c = \frac{V_{faliure}}{V_{total}}, \tag{18}$$

where P_s^c represents the safety index in convex polyhedron reliability models, while P_f^c is the failure index. V_{total} refers to the measurement of the variable space. V_{safe} and $V_{faliure}$ refer to the measurement of the safety region and failure region, respectively.

In the 2-D and 3-D cases shown in Fig. 5, the above indices are measured by area ratio and volume ratio, in which the area of convex polyhedrons can be easily obtained by geometry. In terms of the case of three dimensions or higher dimensions, the calculation of the volume (or hypervolume) of the convex polyhedron can be conducted by the triangulation method or signed decomposition method [46] once the explicit representation of the convex polyhedron is available. Both of the two algorithms decompose the convex polyhedron into a series of n-dimensional simple polyhedrons, each of which consists of $n+1$ vertices. Assume that the $n+1$ vectors of the vertex points of one of the simple polyhedrons are $\mathbf{x}_0, \mathbf{x}_1, \cdots, \mathbf{x}_n$, and the volume of a simple polyhedron can be calculated by

$$V_{simple} = \frac{|\det(\mathbf{x}_1 - \mathbf{x}_0, \cdots, \mathbf{x}_n - \mathbf{x}_0)|}{n!}, \tag{19}$$

where n is the dimension of uncertain variables. Thus the total volume of the original convex polyhedron can be obtained by summing the volume of these simple polyhedrons. The above algorithms have been maturely integrated into MATLAB software, so one can directly call the build-in function "convhulln" to realize the volume calculation. Since the convex polyhedron-related operations belong to the category of geometric mathematics, and the corresponding algorithms have been highly integrated with various software, which can be conveniently utilized for research purpose without own programming, therefore, the algorithm is not detailed in the main article. If readers are interested in the algorithm process, Appendix provides a brief description of the triangulation method for volume calculation of convex polyhedrons. Then the convex polyhedron reliability indices can be calculated by Eqs. (17) and (18).

As for the access to the vertex vectors of convex polyhedrons of the safety region and failure region, it has been stated in Sect. 4.1 that the two expressions of the convex polyhedron can be converted to each other. Hence the vertex vectors required for volume calculation can be obtained based on the closed semi-space representation of the safety region and failure region, i.e., Eq. (16).

4.3 Discussion on the case of the nonlinear limit state function

There are many nonlinear factors in practical engineering, which leads to nonlinear limit state functions. For the general nonlinear limit state function, the limit state line is a curve as shown in Fig. 6, making it difficult to measure the area of the failure region owing to its irregular geometry. To overcome the difficulties, the first-order Taylor expansion is introduced to approximate the limit state function.

For simplicity, the variable space is normalized as follows:

$$x_i' = \frac{x_i - x_i^c}{x_i^r}, \quad i = 1, 2, \cdots, n, \tag{20}$$

where $\mathbf{x}^c = \left(x_1^c, x_2^c, \cdots, x_n^c\right)^T$ is the nominal value of the uncertain variable $\mathbf{x}$ based on given vertices $\{\mathbf{x}^{(1)}, \mathbf{x}^{(2)}, \cdots, \mathbf{x}^{(N)}\}$, which holds

$$x_i^c = \frac{\overline{x}_i + \underline{x}_i}{2}, \quad i = 1, 2, \cdots, n, \tag{21}$$

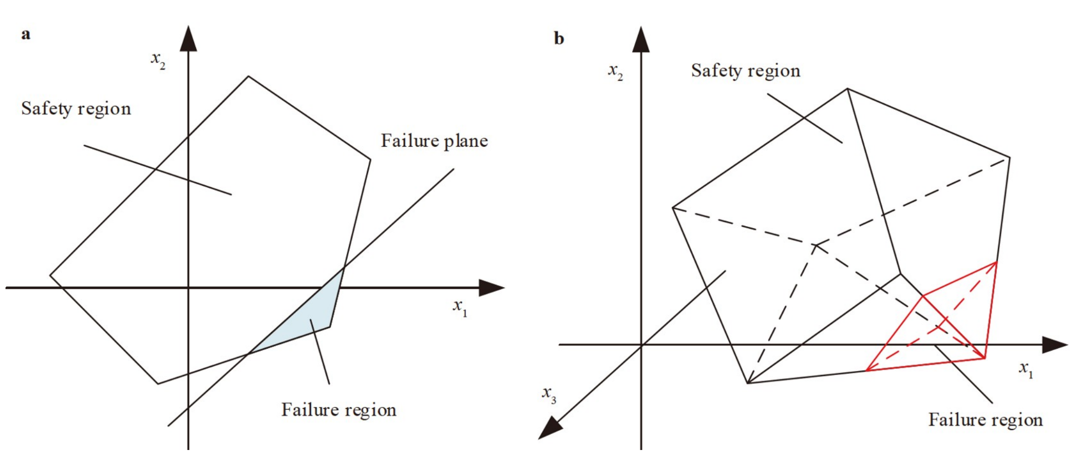

Figure 5 Safety region and failure region in the convex polyhedron reliability model. **a** 2-D reliability; **b** 3-D reliability.

in which

$$\bar{x}_i = \max\left\{x_i^{(1)}, x_i^{(2)}, \cdots, x_i^{(N)}\right\},$$
$$\underline{x}_i = \min\left\{x_i^{(1)}, x_i^{(2)}, \cdots, x_i^{(N)}\right\}. \tag{22}$$

x_i^{r} is the radius of each uncertain variable holding

$$x_i^{\mathrm{r}} = \frac{1}{2}(\bar{x}_i - \underline{x}_i), \quad i = 1, 2, \cdots, n. \tag{23}$$

After the transformation, the limit state function is rewritten as

$$g'(\mathbf{x}') = g\left(x_1^{\mathrm{r}} x_1' + x_1^{\mathrm{c}}, x_2^{\mathrm{r}} x_2' + x_2^{\mathrm{c}}, \cdots, x_n^{\mathrm{r}} x_n' + x_n^{\mathrm{c}}\right). \tag{24}$$

Then Taylor's series expansion of $g'(\mathbf{x}')$ is taken at the most likely failure point $\mathbf{x}^*$, which is defined as the closest point to the origin of $\mathbf{x}'$- coordinate on the limit state curve. The most likely failure point can be obtained by solving the following optimization problem.

$$\begin{aligned} &\text{find } \mathrm{x}', \\ &\min \|\mathbf{x}'\|^2 = \sum_{i=1}^{n} (x'_i)^2, \\ &\text{s.t. } g'(\mathbf{x}') = 0. \end{aligned} \tag{25}$$

In this work, Hasofer-Lind and Rackwitz-Fiessler (HL-RF) iteration method [47,48] is used to solve Eq. (25). The iteration scheme is given as follows:

$$d^{(k)} = \frac{g'(\mathbf{x}'^{(k)}) - \left[\nabla g'(\mathbf{x}'^{(k)})\right]^{\mathrm{T}} \mathbf{x}'^{(k)}}{\left\|\nabla g'(\mathbf{x}'^{(k)})\right\|},$$
$$\mathbf{x}'^{(k+1)} = -d^{(k)} \frac{\nabla g'(\mathbf{x}'^{(k)})}{\left\|\nabla g'(\mathbf{x}'^{(k)})\right\|}, \tag{26}$$

where

$$\nabla g'(\mathbf{x}') = \left[\frac{\partial g'(\mathbf{x}')}{\partial \mathbf{x}'}\right]^{\mathrm{T}} = \left[\frac{\partial g'(\mathbf{x}')}{\partial x'_1}, \frac{\partial g'(\mathbf{x}')}{\partial x'_2}, \cdots, \frac{\partial g'(\mathbf{x}')}{\partial x'_n}\right]^{\mathrm{T}}. \tag{27}$$

After acquiring the most likely failure point $\mathbf{x}^*$, taking the first-order Taylor's series expansion of $g'(\mathbf{x}')$ at $\mathbf{x}^*$ yields

$$M = g'(\mathbf{x}') \approx g'(\mathbf{x}^*) + \sum_{i=1}^{n} \frac{\partial g'}{\partial x_i^*}(x_i^* - x'_i). \tag{28}$$

Thus the linear approximation of the weak nonlinear limit state surface can be expressed as follows:

$$g'(\mathbf{x}^*) + \sum_{i=1}^{N} \frac{\partial g'}{\partial x_i^*} \Delta x_i^* = 0. \tag{29}$$

Then, based on linearized limit state surface Eq. (29), the method for the case of linear limit state functions provided in Sect. 4.2 can be adopted to conduct the convex polyhedron reliability analysis.

In view of general cases, if the limit state function has strong nonlinearity, as shown in Fig. 7, the above Taylor's series expansion-based linearization method may lead to unacceptable errors. In order to overcome the difficulty, a piecewise linearization method is presented to approximate the strong nonlinear limit state function.

Figure 8 shows the nonlinear limit state surface approximation by the piecewise linearization method with several

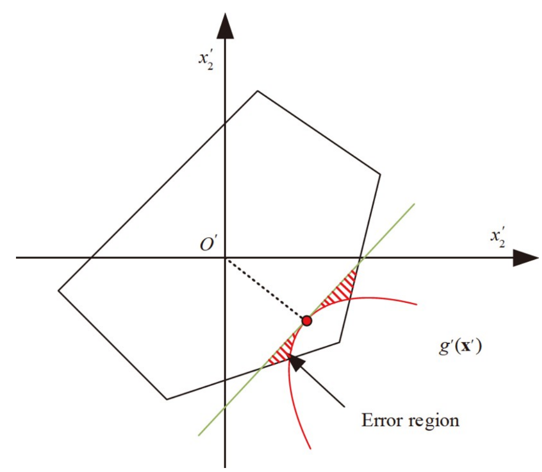

Figure 7 Error caused by linear approximation.

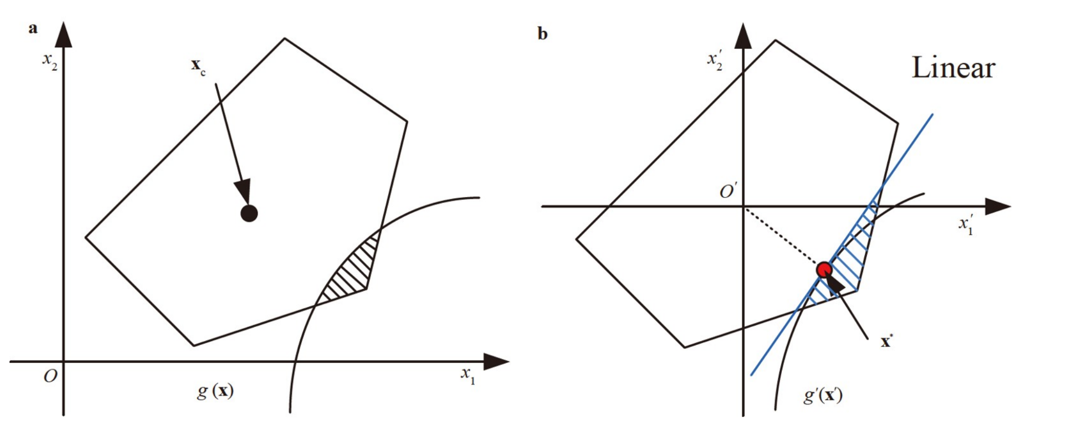

Figure 6 Nonlinear limit state function and its linear approximation. **a** Nonlinear limit state function; **b** approximation in normalized space.

line segments. It can be seen that the nonlinear limit state surface and the convex polyhedron boundary intersect at $\mathbf{x}^1, \mathbf{x}^2$. The tangents l_1, l_2, l_3 at $\mathbf{x}^1, \mathbf{x}^2, \mathbf{x}^*$ are obtained by Taylor's series expansion, respectively. $\mathbf{x}^3, \mathbf{x}^4$ are the intersection of l_3, l_1, and l_2, respectively. Then the failure region and safety region in this 2-D case can be described by convex polyhedrons constructed by vertices $\mathbf{x}_1^{\mathrm{v}}, \mathbf{x}_2^{\mathrm{v}}, \cdots, \mathbf{x}_N^{\mathrm{v}}$ and $\mathbf{x}^*, \mathbf{x}^1, \mathbf{x}^2, \mathbf{x}^3, \mathbf{x}^4$.

The above discussion is suitable for 2-D cases. In higher dimensional cases, it is difficult to catch the intersection, but the piecewise linearization method proposed in this paper can still be extended to high-dimensional strong nonlinear cases. A possible treatment is collecting a point set on failure surface, i.e., $\Pi_{\mathrm{x}} = \{\mathbf{x}^*, \mathbf{x}^1, \mathbf{x}^2, \cdots\}$ satisfying $g'(\mathbf{x}^i) = 0,\ i = 1, 2, \cdots$. Then taking Taylor's series expansion yields the linear approximation of failure surface as follows. The extend strong nonlinear limited state function (LSF) piecewise linearization method in 2-D and 3-D are shown in Fig. 9.

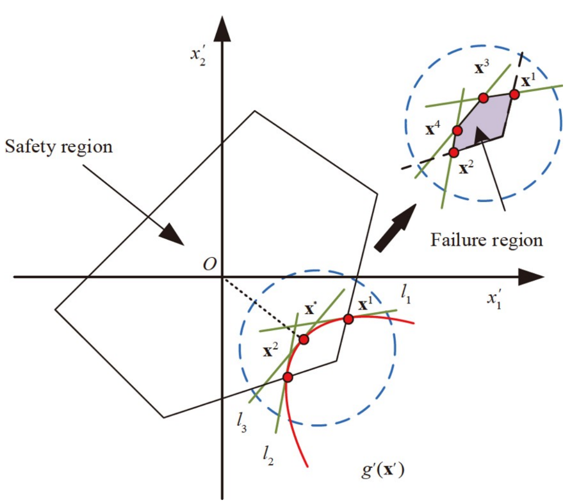

Figure 8 Piecewise linearization for the nonlinear limit state function.

$$\begin{cases} g'(\mathbf{x}^*) + \sum_{i=1}^{N} \dfrac{\partial g'}{\partial x_i^*} \Delta x_i^* = 0, \\ g'(\mathbf{x}^1) + \sum_{i=1}^{N} \dfrac{\partial g'}{\partial x_i^1} \Delta x_i^1 = 0, \\ g'(\mathbf{x}^2) + \sum_{i=1}^{N} \dfrac{\partial g'}{\partial x_i^2} \Delta x_i^2 = 0, \\ \dots \end{cases} \tag{30}$$

If the original failure surface is convex, the overlap of the failure or safety regions based on failure planes in Eq. (30) forms a convex polyhedron, which is the approximation of the original failure or safety region. In theory, the more points utilized, the more accurate the approximation. It is noted that this subsection only discusses a preliminary idea, and detailed studies will be carried out in the future.

5. Convex polyhedron reliability analysis for structural system problems with multiple failure modes

The reliability analysis of structural systems has attracted great attention from researchers. When it comes to the case of multiple failure modes, because of the difficulty of reliability solving due to the correlation between the main failure modes, the conservative but straightforward treatment method is to ignore the correlation directly, which will lead to a large error in reliability evaluation. Given this, this paper proposes a failure region superposition method to deal with the correlation of multiple failure modes, and it can get more accurate reliability evaluation results.

In engineering structures, there always exist various correlations between failure modes, of which the influence must be considered. In this section, we suppose that the

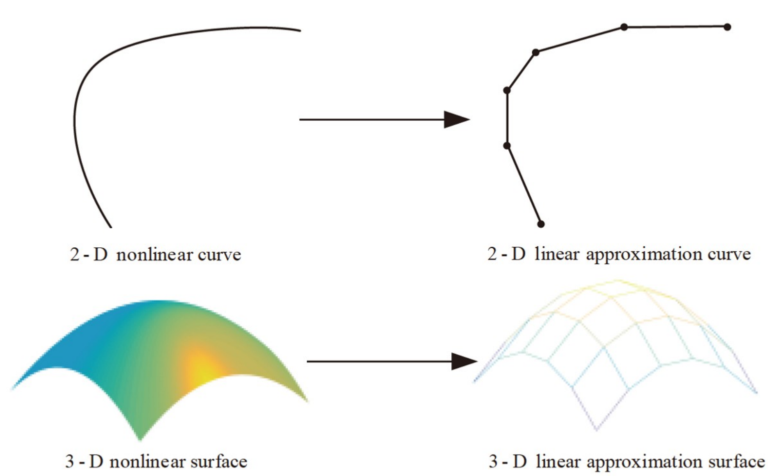

Figure 9 Extend strong nonlinear LSF piecewise linearization method in 2-D and 3-D.

correlated limit state functions of the i-th and j-th failure modes are expressed by $M_i(R_1, R_2)$ and $M_j(R_1, R_2)$, in which the correlated variables are R_1 and R_2.

In general, we should calculate the hybrid correlation coefficient of two failure modes and the second-order joint failure probability of two failure modes to obtain the reliability of the entire structural system, as discussed by Qiu and Wang [49]. However, calculating the hybrid correlation coefficient and joint failure probability will be a challenge in multiple failure modes. This paper presents a convex polyhedron reliability analysis method for structures with correlated failure modes based on the mixed failure region.

Assuming that uncertain variables in M_i and M_j are R_1 and R_2, we can accordingly obtain the failure region for each failure mode. The failure plane corresponding to failure modeM_i divides the variable space into failure region and safety region as shown in Fig. 10. Considering only the failure mode M_i, the structural failure index is

$$P_{fi} = \frac{V_{fi}}{V_{total}}, \tag{31}$$

where V_{fi} represents the area or volume of failure region in the failure mode M_i.

Similarly, considering only the failure mode M_j, the structural failure index is

$$P_{fj} = \frac{V_{fj}}{V_{total}}, \tag{32}$$

where V_{fj} represents the area or volume of failure region in the failure mode M_j.

Considering the two failure modes simultaneously, we discuss the parallel system and series system [50], respectively. Here we only consider linear cases, assuming that

$$M_i = a_{0i} + \mathbf{a}_i^{\mathrm{T}}\mathbf{R}, \tag{33}$$

$$M_j = a_{0j} + \mathbf{a}_j^{\mathrm{T}}\mathbf{R}. \tag{34}$$

For parallel systems, the structural system fails only if both failure modes are activated. Hence, the failure region of the structural system is the intersection of the failure regions of two failure modes, namely, $\Omega_{fparallel} = \Omega_{fi} \cap \Omega_{fj}$. As shown in Fig. 11a, the failure region is a convex polyhedron. According to Eq. (16), the convex polyhedron of $\Omega_{fparallel}$ can be expressed as

$$\Omega_{fparallel} = \left\{ \mathbf{x} \in \mathbf{R}^2 \left| \begin{bmatrix} \mathbf{A} \\ \mathbf{a}_i^{\mathrm{T}} \\ \mathbf{a}_j^{\mathrm{T}} \end{bmatrix} \mathbf{x} \le \begin{bmatrix} \mathbf{b} \\ -a_{0i} \\ -a_{0j} \end{bmatrix} \right. \right\}. \tag{35}$$

And its area or volume $V_{fparallel}$ can be calculated by the approach for convex polyhedrons, as stated in Sect. 4. Then the failure index is able to be calculated by

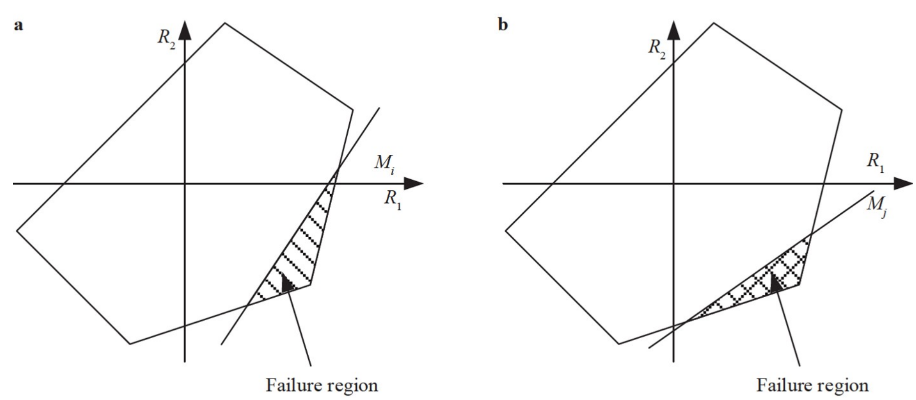

Figure 10 Failure region of single failure modes. **a** Failure region under mode M_i; **b** failure region under mode M_j.

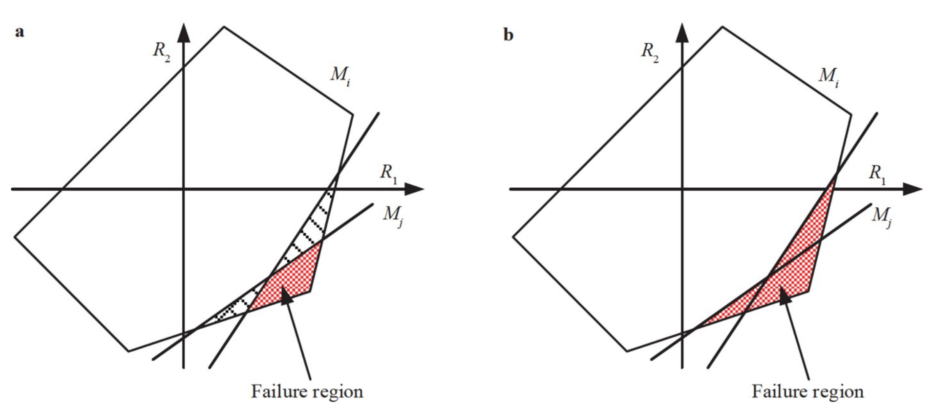

Figure 11 Failure region in the case of multiple failure modes. **a** Failure region for parallel systems; **b** failure region for series systems.

$$P_{\text{fparallel}} = \frac{V_{\text{fparallel}}}{V_{\text{total}}}. \tag{36}$$

For series systems, the structural system fails once any of the failure modes is triggered. As shown in Fig. 11b, the failure region of the structural system is the union of the failure regions of multiple failure modes, i.e., $\Omega_{\text{fparallel}} = \Omega_{\text{f}i} \cup \Omega_{\text{f}j}$. In such circumstance, $\Omega_{\text{fparallel}}$ is not a convex polyhedron, but the safe region is a convex polyhedron holding

$$\Omega_{\text{sseries}} = \left\{ \mathbf{x} \in \mathbf{R}^2 \left| \begin{bmatrix} \mathbf{A} \\ -\mathbf{a}_i^{\text{T}} \\ -\mathbf{a}_j^{\text{T}} \end{bmatrix} \mathbf{x} \le \begin{bmatrix} \mathbf{b} \\ a_{0i} \\ a_{0j} \end{bmatrix} \right. \right\}. \tag{37}$$

After the representation of the convex polyhedron is obtained, one can calculate its area or volume V_{sseries}. The failure index can be calculated by

$$P_{\text{fseries}} = 1 - P_{\text{sseries}} = 1 - \frac{V_{\text{sseries}}}{V_{\text{total}}}. \tag{38}$$

Similarly, considering multiple failure modes and high dimensional cases, the above can be simply extended, namely, $\Omega_{\text{fparallel}} = \Omega_{\text{f}1} \cap \Omega_{\text{f}2} \cap \cdots \cap \Omega_{\text{f}n}$ for parallel systems and $\Omega_{\text{sseries}} = \Omega_{\text{s}1} \cup \Omega_{\text{s}2} \cup \cdots \cup \Omega_{\text{s}n}$ for series systems. Note that the hybrid systems simultaneously involving parallel and series relations are not discussed in this paper.

6. Numerical and engineering examples

In this section, to demonstrate the effectiveness and accuracy of the proposed convex polyhedron reliability method, one numerical example and two engineering examples are provided.

6.1 Numerical example with a linear limit state function

In this section, we use a numerical example to demonstrate the efficiency and validity of the present non-probabilistic convex polyhedron safety measurement.

We consider a general limit state function as follows:

$$M(r,s) = r - s, \tag{39}$$

where r, s represents general structural strength and general structural stress, respectively.

For comparison, the probabilistic reliability analysis model is first investigated. It is assumed that the distribution of two variables follows the truncated normal probabilistic density function, namely

$$f_{\text{joint}}(r,s) = c\exp\left\{ -\frac{[(s-S^{\text{c}})\cos\theta - (r-R^{\text{c}})\sin\theta]^2}{a^2} - \frac{[(s-S^{\text{c}})\sin\theta + (r-R^{\text{c}})\cos\theta]^2}{b^2} \right\}, \tag{40}$$

when $|r-R^{\text{c}}| \le R^{\text{r}}$, $|s-S^{\text{c}}| \le S^{\text{r}}$, and

$$f_{\text{joint}}(r,s) = 0, \tag{41}$$

when $|r-R^{\text{c}}| > R^{\text{r}}$ or $|s-S^{\text{c}}| > S^{\text{r}}$. c is the normalization constant by which the following relationship is held:

$$\int_{S^{\text{c}}-S^{\text{r}}}^{S^{\text{c}}+S^{\text{r}}} \int_{R^{\text{c}}-R^{\text{r}}}^{R^{\text{c}}+R^{\text{r}}} f_{\text{joint}}(r,s)\text{d}r\text{d}s = 1. \tag{42}$$

θ is the off-axis angle, and a, b are variance-dependent parameters.

We set the parameters in Eq. (40) as $\theta = 45°$, $R^{\text{c}} = 5$, $R^{\text{r}} = 2.5$, $S^{\text{c}} = 4.5$, $S^{\text{r}} = 2.5$. Figure 12 shows the probabilistic density function of random variables.

Based on Eq. (2), the failure probability of Eq. (39) can be obtained.

$$P_{\text{f}} = \iint_{\Omega_{\text{f}}} f_{\text{joint}}(r,s)\text{d}r\text{d}s = 0.3029. \tag{43}$$

Next, the non-probabilistic reliability models are discussed. Suppose that the probabilistic density function Eqs. (40) and (41) reflects the real probabilistic distribution of the uncertain variables, and then 100 sample points are generated, by which the convex polyhedron model is established. For comparison, some other available non-probabilistic models are also established in this example, including the interval model, ellipsoid model, and rectangle MP model [40].

It is notable that the purpose of the above treatment is to imitate the situation where the number of sample points is limited and not enough to determine the probabilistic characteristics in practical engineering. Therefore, considering such practical situation of limited data, the non-probabilistic reliability models are adopted. Then, considering the ideal situation of adequate data, the probabilistic reliability is calculated by Eqs. (40) and (41) and referred to as the actual reliability for comparison. Through such comparison with a

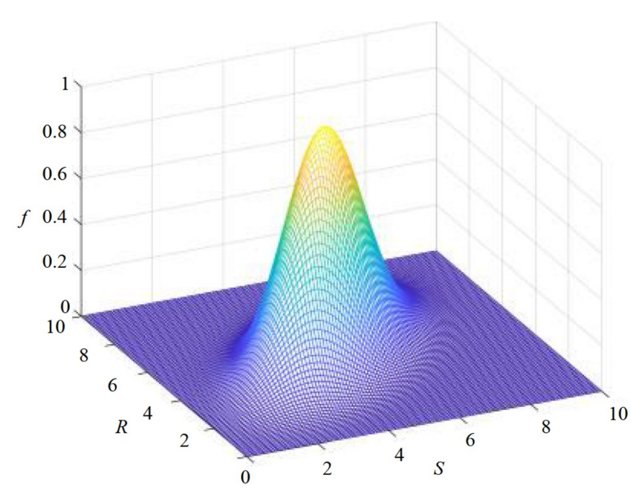

Figure 12 Probabilistic density function of random variables R and S.

reference standard, we can evaluate the performance of different non-probabilistic models more reasonably and intuitively.

Figure 13 shows the difference between the convex polyhedron reliability model and other non-probabilistic models. In virtue of the area ratio, we can calculate the failure indices of different non-probabilistic models. The failure index of the convex polyhedron reliability analysis model is $P_f^c = V_{\text{failure}} / V_{\text{total}} = 0.3238$. In the same way, the failure indices of the interval model, ellipsoid model, and rectangle MP model are $P_f^I = 0.3930$, $P_f^E = 0.3885$, and $P_f^{RMP} = 0.2850$, respectively.

Since the generation of sample points has randomness, 10 simulations are carried out to illustrate the performance of the provided models more reasonably. The results are listed in Table 1 and discussed as follows.

In most situations, the relationship between the failure indices of interval and convex polyhedron models satisfies

$$P_f^I > P_f^c. \tag{44}$$

It can be seen that the reliability assessed by the interval model is more conservative than that of the convex polyhedron model.

As for ellipsoid model and rectangle MP model, which are also constructed considering correlation, the relationship between convex polyhedron and ellipsoid models holds

$$P_f^E > P_f^c. \tag{45}$$

From Fig. 13 we can observe that the convex polyhedron model is more refined than ellipsoid model, therefore explaining the relationship (45). Meanwhile, no specific regularity appears in the relationship between the rectangle MP reliability model and convex polyhedron model or ellipsoid model. Nevertheless, since the correlation is considered, it is obviously that the reliability assessed by convex polyhedron, ellipsoid and rectangle MP models is less conservative than that of interval model, i.e., $P_f^I > P_f^c$, $P_f^I > P_f^E$ and $P_f^I > P_f^{RMP}$.

As shown in Table 1, on average, the relationship between the convex polyhedron model and other models satisfies

$$P_{f,\text{ave}}^I > P_{f,\text{ave}}^E > P_{f,\text{ave}}^{RMP} > P_{f,\text{ave}}^c, \tag{46}$$

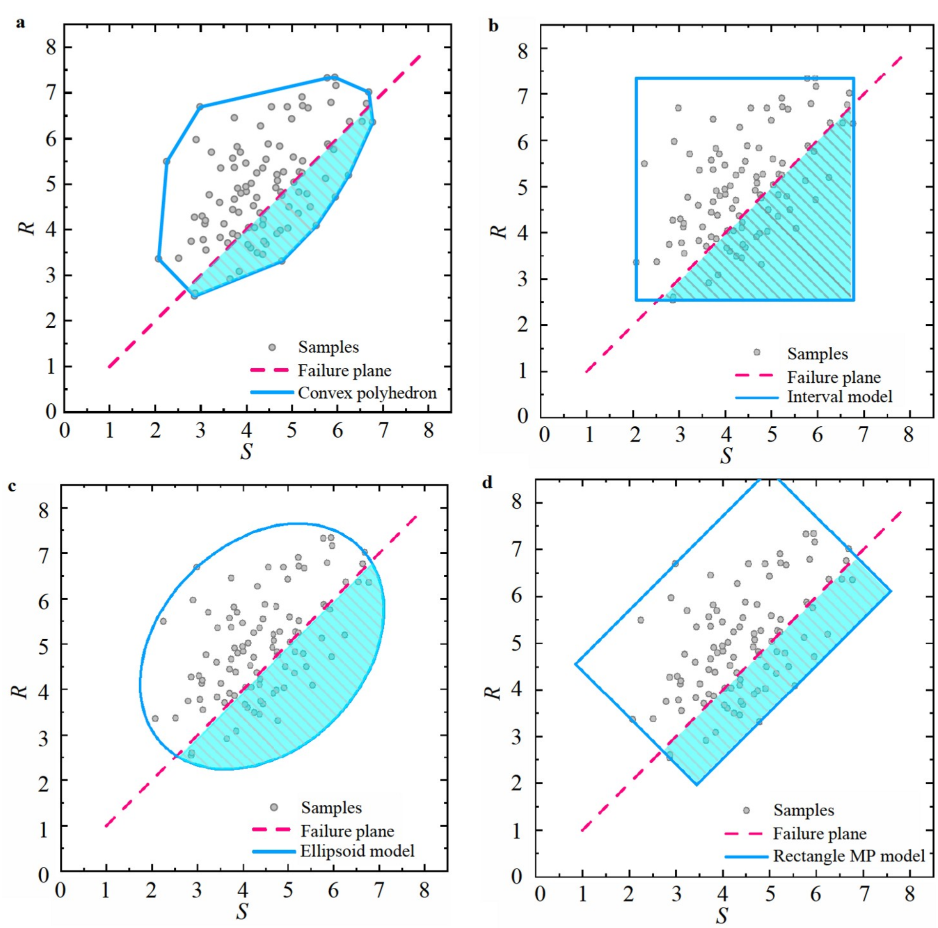

Figure 13 Comparison of different non-probabilistic reliability models. **a** Interval reliability model; **b** convex polyhedron reliability model; **c** ellipsoid reliability model; **d** rectangle MP reliability model.

Table 1 Results from 10 simulations

Sequence	Convex polyhedron		Interval		Ellipsoid		Rectangle MP	
	P_f^c	Deviation (%)	P_f^I	Deviation (%)	P_f^E	Deviation (%)	P_f^{RMP}	Deviation (%)
1	0.3688	21.76	0.4249	40.28	0.3885	28.26	0.2850	5.91
2	0.3163	4.42	0.3886	28.29	0.3434	13.37	0.3105	2.51
3	0.3040	0.36	0.4238	39.91	0.3995	31.89	0.2945	2.77
4	0.3185	5.15	0.3896	28.62	0.3592	18.59	0.3633	19.94
5	0.3535	16.70	0.4169	37.64	0.3723	22.91	0.3917	29.32
6	0.3282	8.35	0.4240	39.98	0.4154	37.14	0.3522	16.28
7	0.2996	1.09	0.4076	34.56	0.3894	28.56	0.3130	3.33
8	0.3112	2.74	0.3986	31.59	0.3530	16.54	0.3766	24.33
9	0.3582	18.26	0.4136	36.55	0.3998	31.99	0.3968	31.00
10	0.2694	11.06	0.3830	26.44	0.3298	8.88	0.2800	7.56
Average	0.3228	6.56	0.4071	34.39	0.3750	23.81	0.3364	11.05

where the average deviations of P_f^I, P_f^E, P_f^{RMP}, P_f^c are 34.39%, 23.81%, 11.05%, 6.56%, respectively. The comparison indicates that, in the case of a limited sample size, the non-probabilistic convex polyhedron reliability is more consistent with the actual reliability. Although the results of convex polyhedron model and rectangle MP model are similar on average, the latter shows obvious fluctuation in single calculations.

In general, it is evident that the reliability evaluated by non-probabilistic models is more conservative than probabilistic reliability because the former merely utilizes limited information while the latter takes advantage of adequate information. This phenomenon also illustrates the compatibility between the reliability evaluated by probabilistic and non-probabilistic models. When data are adequate and the probabilistic distribution can be obtained, the probabilistic reliability analysis model is the best way to precisely evaluate the structural reliability. If data are limited and the probabilistic distribution is unavailable, the non-probabilistic reliability analysis model will be a practicable reliability analysis approach to provide the more conservative assessment for structural safety.

6.2 Cantilever beam structure with a nonlinear limit state function

As shown in Fig. 14, a cantilever beam is investigated in this example. The external loads in this model are P_z = 50000 N and P_y = 25000 N.

The maximum stress at the fixed end of the beam should be less than the yield strength S, and then a limit state function can be derived as follows:

$$g(\mathbf{X}) = S - \frac{6P_zL}{b^2h} - \frac{6P_yL}{bh^2}, \tag{47}$$

where L, b and h are treated as uncertain variables with

Table 2 Information of uncertain variables

Parameter	Intervals
L	[900 mm, 1100 mm]
b	[90 mm, 110 mm]
h	[180 mm, 220 mm]

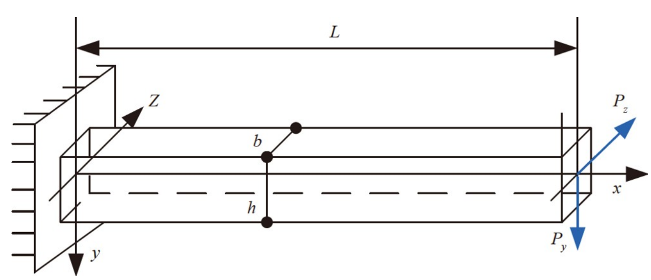

Figure 14 Cantilever beam.

intervals as listed in Table 2. Sample points are randomly generated to construct the convex polyhedron models.

Figure 15 shows the convex polyhedron and nonlinear failure plane. The black dots represent the sample points that generate the convex polyhedron, and the red surface is the nonlinear failure surface.

The limit state function Eq. (47) is a nonlinear limit state function. Therefore, we transform the nonlinear limit state function to a linear limit state function using Eqs. (24) and (29) as stated in Sect. 4.3. First, the coordinate transformation is conducted as follows:

$$g'(\mathbf{x}') = S - \frac{6P_z(L'+L_c)}{(b'+b_c)^2(h'+h_c)} - \frac{6P_y(L'+L_c)}{(b'+b_c)(h'+h_c)^2}. \tag{48}$$

And the linear limit state function can be written as

$$\bar{g}'(\mathbf{x}') = g'(\mathbf{x}^*) + \frac{\partial g'(\mathbf{x}')}{\partial L'}\Delta L' + \frac{\partial g'(\mathbf{x}')}{\partial b'}\Delta b' + \frac{\partial g'(\mathbf{x}')}{\partial h'}\Delta h', \tag{49}$$

where the terms are expressed as follows:

$$
\begin{aligned}
&g'(\mathbf{x}^*) = S - \frac{6P_z L^*}{(b^*)^2 h^*} - \frac{6P_y L^*}{b^*(h^*)^2},\\
&\frac{\partial g'(\mathbf{x}')}{\partial L'} = \left[-\frac{6P_z}{(b'+b_c)^2(h'+h_c)} - \frac{6P_y}{(b'+b_c)(h'+h_c)^2}\right]\Bigg|_{\mathbf{X}^*},\\
&\qquad \Delta L' = L' - L^*,\\
&\frac{\partial g'(\mathbf{x}')}{\partial b'} = \left[\frac{12P_z(L'+L_c)}{(b'+b_c)^3(h'+h_c)} + \frac{6P_y(L'+L_c)}{(b'+b_c)^2(h'+h_c)^2}\right]\Bigg|_{\mathbf{X}^*},\\
&\qquad \Delta b' = b' - b^*,\\
&\frac{\partial g'(\mathbf{x}')}{\partial h'} = \left[\frac{6P_z(L'+L_c)}{(b'+b_c)^2(h'+h_c)^2} + \frac{12P_y(L'+L_c)}{(b'+b_c)(h'+h_c)^3}\right]\Bigg|_{\mathbf{X}^*},\\
&\qquad \Delta h' = h' - h^*.
\end{aligned}
\tag{50}
$$

Failure region and safety region are shown in Fig. 16. $g'(\mathbf{x}')$ and $\overline{g'}(\mathbf{x}')$ are nonlinear and linear limit state functions, respectively. The most likely failure point is calculated by Eq. (25). As can be seen from Fig. 16, $g'(\mathbf{x}')$ and $\overline{g'}(\mathbf{x}')$ are very close, indicating that the linear approximation of $g'(\mathbf{x}')$ is reasonable. Then the convex polyhedron reliability of the cantilever beam can be calculated as

$$
P_s = \frac{V_{\text{safe}}}{V_{\text{total}}} = \frac{13.4841}{13.6001} = 99.15\%. \tag{51}
$$

6.3 A wing structure with multiple failure modes

In order to verify the performance of the proposed method in practical engineering, this example considers a wing structure shown in Fig. 17. The external pressure p, elasticity modulus E, skin thickness t_{skin}, beam thickness t_{beam}, and rib thickness t_{rib} are considered as uncertain variables.

It is treated in the same way as example 1 that an ideal situation is first supposed where the uncertain variables are of the known truncated normal distribution listed in Table 3, where α is the variance factor.

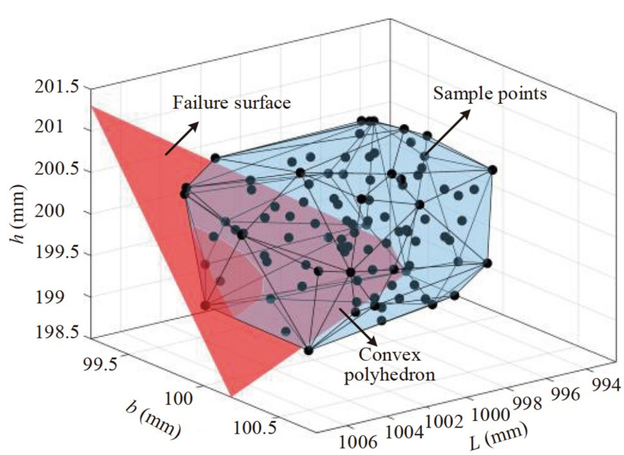

Figure 15 Uncertain variable space and nonlinear failure surface.

Under such an ideal circumstance, one can directly assess the reliability via probabilistic models. However, in practice, available data are limited, and the ideal situation where the probabilistic distribution is known is generally difficult to achieve. To simulate the situation where the available data are limited and probabilistic distribution is unknown, in this example, we generate a small number of samples through the probabilistic distribution in the ideal situation as available limited data. Then only these limited data are used for reliability analysis with non-probabilistic models involving the convex polyhedron model and interval model.

There are two main failure criteria that the maximum stress and maximum displacement must be below the allowable values, which are set as $\sigma_0 = 275$ MPa and $u_0 = 13$ mm, respectively, in this example.

$$
\begin{aligned}
M_1 &= \sigma_0 - \sigma_{\max}(p, E, t_{\text{skin}}, t_{\text{beam}}, t_{\text{rib}}),\\
M_2 &= u_0 - u_{\max}(p, E, t_{\text{skin}}, t_{\text{beam}}, t_{\text{rib}}).
\end{aligned}
\tag{52}
$$

Table 3 The uncertain information of variables

	p (Pa)	E (Mpa)	t_{skin} (mm)	t_{beam} (mm)	t_{rib} (mm)
Mean value	17	110	2	2	2
Standard deviation	1α	10α	0.1α	0.1α	0.1α

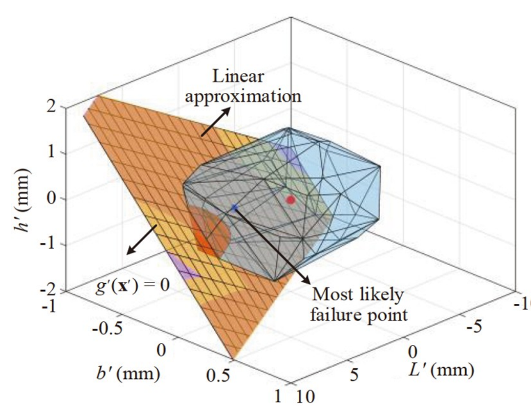

Figure 16 Approximate linear failure surface and failure region.

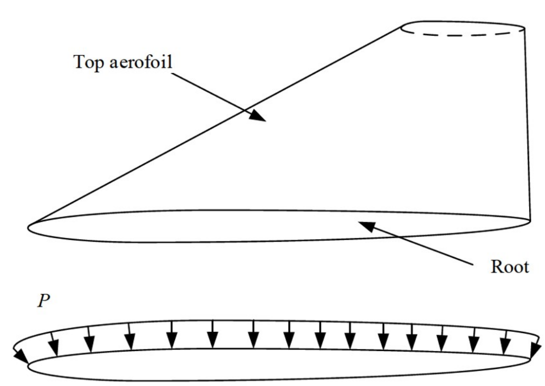

Figure 17 Wing structure with fixed root.

The maximum stress and maximum displacement are calculated by the finite element method. As shown in Fig. 18, a FE model with 6297 nodes and 8164 elements is created to carry out the structural analysis.

Further, in order to evaluate the practical utility and rationality of the reliability calculated by non-probabilistic models, we employ the probabilistic reliability in the ideal case as a standard for comparison.

The safety reliability and failure reliability estimated by the three models with respect to the variance factor are plotted in Figs. 19 and 20, respectively. From the results, we can see that with the increase of the variance factor, the safety reliability index decreases and the failure reliability index increases. More importantly, the curves have shown that the convex polyhedron reliability fits better with the standard probabilistic reliability with a maximum error of 0.64%. Moreover, the reliability evaluated by the convex polyhedron model is always more conservative than that of the truncated probabilistic model.

In view of the interval model, with the variance factor increasing, the deviation between the interval model and the truncated probabilistic model becomes larger. Moreover, since the correlation is not taken into account, the reliability obtained by the interval model is much more conservative.

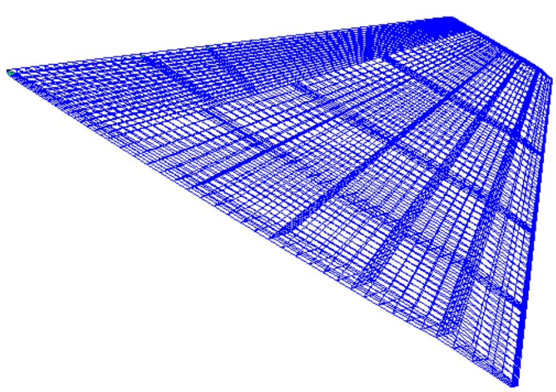

Figure 18 Finite element model of the wing structure.

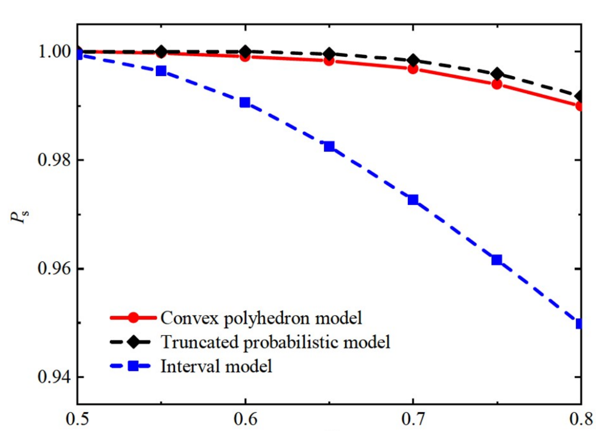

Figure 19 Safety index of the three models versus α.

In summary, on the one hand, this example verifies the applicability of the proposed convex polyhedron reliability model in engineering structures with multiple failure modes. On the other hand, the reliability is evaluated under two kinds of cases. In the ideal case, the probabilistic distribution is given and the probabilistic reliability is calculated as a reference solution. In the case of limited data, the probabilistic distribution is unknown and non-probabilistic models are implemented for reliability analysis using these limited data. By comparison, the performance of the adopted non-probabilistic models is illustrated. Besides, since the uncertainty exists objectively, the reliability evaluated by different models should be compatible. The comparison also supports this viewpoint.

7. Conclusions

In this paper, considering the limitations of high demand on the original data for the probabilistic reliability model and the overly rough estimation of the interval reliability model, a convex polyhedron-based reliability analysis model is proposed. The non-probabilistic convex polyhedron model is introduced to describe the uncertainties with correlation, and the reliability is quantified via the measurement ratios of the safety region, safety region, and total region. In terms of nonlinear limit state functions, this paper provides the most likely failure point-based linearization method and the piecewise linearization method to deal with weak and strong nonlinear problems, respectively. Further, the system reliability analysis method for structures with multiple failure modes is studied based on the proposed convex polyhedron reliability model. Under the same situation of limited data, compared with the interval model, the convex polyhedron model envelopes the uncertainties with a MCP instead of an interval, reducing the uncertain variable space by considering the correlation. Therefore, the reliability evaluated by the proposed method will be more consistent with the actual situation than that of interval reliability models.

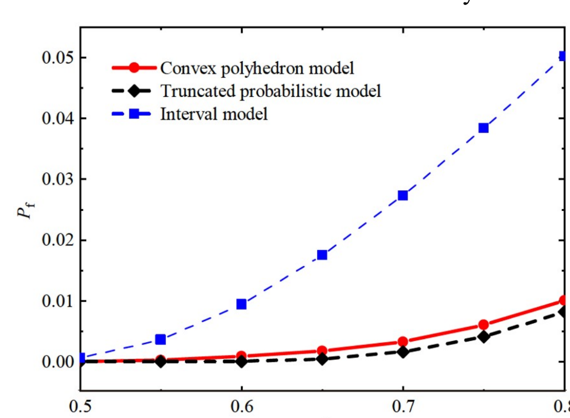

Figure 20 Failure index of the three models versus α.

Finally, three examples are provided to demonstrate the performance of the proposed reliability analysis model. The first example verifies the validity of the proposed method by a linear numerical example, in which the probabilistic reliability is supposed to be the actual reliability. The proposed method, the interval, ellipsoid, and rectangle MP models are employed to assess the reliability based on limited data generated via the probabilistic distribution. The comparing results show that the non-probabilistic reliability is more conservative than the probabilistic reliability, indicating the compatibility, and the convex polyhedron reliability is more consistent with the actual reliability. The second example tests the proposed method by a cantilever beam structure with a nonlinear limit state function, demonstrating the ability of the proposed method to address the nonlinearity. In order to verify the applicability of the proposed method to engineering structures, a wing structure with multiple failure modes is studied in the third example. The probabilistic reliability model, the interval reliability model, and the proposed convex polyhedron reliability model are adopted to evaluate the system reliability of the wing structure under different variance factors. The comparison indicates that the convex polyhedron reliability is always similar to the probabilistic reliability and more conservative, illustrating the rationality and applicability of the proposed convex polyhedron reliability model. Noting that this paper mainly implements a study on the non-probabilistic convex polyhedron reliability model under the linear or weakly nonlinear cases, along with a preliminary discussion on treatment in strongly nonlinear cases, so it is still necessary to study strongly nonlinear problems in more detail in the future.

Author contributions *Zhiping Qiu designed the research. Haijun Tang wrote the first draft of the manuscript. Haijun Tang set up the experiment set-up and processed the experiment data. Bo Zhu helped organize the manuscript. Bo Zhu and Haijun Tang revised and edited the final version.*

Acknowledgements *This work was supported by the Defense Industrial Technology Development Program (Grant Nos. JCKY2018601B001, JCKY2019209C004, and JCKY2019205A006), the National Natural Science Foundation of China (Grant Nos. 11432002, 11772026, and 12002015), the Aeronautical Science Foundation of China (Grant No. 20182951014), and the Beijing Municipal Science and Technology Commission (Grant No. Z191100004619006). The authors also express appreciation to the anonymous reviewers and the editors for their valuable comments and suggestions.*

1 Y. Zheng, D. Da, H. Li, M. Xiao, and L. Gao, Robust topology optimization for multi-material structures under interval uncertainty, Appl. Math. Model. **78**, 627 (2020).

2 D. Maruyama, P. Bekemeyer, S. Görtz, S. Coggon, and S. Sharma, Data-driven Bayesian inference of turbulence model closure coefficients incorporating epistemic uncertainty, Acta Mech. Sin. **37**, 1812 (2022).

3 C. Jiang, J. Zheng, and X. Han, Probability-interval hybrid uncertainty analysis for structures with both aleatory and epistemic uncertainties: A review, Struct. Multidisc. Optim. **57**, 2485 (2018).

4 Z. Qiu, and B. Zhu, A Newton iteration-based interval analysis method for nonlinear structural systems with uncertain-but-bounded parameters, Int. J. Numer. Methods Eng. **122**, 4922 (2021).

5 I. Elishakoff, Three versions of the finite element method based on concepts of either stochasticity, fuzziness, or anti-optimization, Appl. Mech. Rev. **51**, 209 (1998).

6 J. W. R. Meggitt, and A. T. Moorhouse, A covariance based framework for the propagation of correlated uncertainty in frequency based dynamic sub-structuring, Mech. Syst. Signal Process. **136**, 106505 (2020).

7 L. Hu, R. Kang, X. Pan, and D. Zuo, Uncertainty expression and propagation in the risk assessment of uncertain random system, IEEE Syst. J. **15**, 1604 (2021).

8 Q. F. Lü, W. Q. Zhu, and M. L. Deng, Reliability of quasi integrable and non-resonant Hamiltonian systems under fractional Gaussian noise excitation, Acta Mech. Sin. **36**, 902 (2020).

9 L. Campioni, and P. Vestrucci, Monte Carlo importance sampling optimization for system reliability applications, Ann. Nucl. Energy **31**, 1005 (2004).

10 H. P. Gavin, and S. C. Yau, High-order limit state functions in the response surface method for structural reliability analysis, Struct. Saf. **30**, 162 (2008).

11 T. Zhang, and M. Xie, On the upper truncated Weibull distribution and its reliability implications, Reliability Eng. Syst. Saf. **96**, 194 (2011).

12 X. Du, and Z. Hu, First order reliability method with truncated random variables, J. Mech. Des. **134**, 091005 (2012).

13 F. Zhang, X. Xu, L. Cheng, S. Tan, W. Wang, and M. Wu, Mechanism reliability and sensitivity analysis method using truncated and correlated normal variables, Saf. Sci. **125**, 104615 (2020).

14 Y. Ben-Haim, and I. Elishakoff, Convex Models of Uncertainty in Applied Mechanics (Elsevier, Amsterdam, 1990).

15 I. Elishakoff, Essay on uncertainties in elastic and viscoelastic structures: From A. M. Freudenthal's criticisms to modern convex modeling, Comput. Struct. **56**, 871 (1995).

16 B. Jia, Z. Lu, and J. Lei, Fuzzy first-order and second moment method for failure credibility analysis in the presence of fuzzy uncertainty, IEEE Trans. Fuzzy Syst. **30**, 3166 (2022).

17 L. F. You, J. G. Zhang, S. Zhou, and J. Wu, A novel mixed uncertainty support vector machine method for structural reliability analysis, Acta Mech. **232**, 1497 (2021).

18 M. Bagheri, S. P. Zhu, M. E. A. Ben Seghier, B. Keshtegar, and N. T. Trung, Hybrid intelligent method for fuzzy reliability analysis of corroded X100 steel pipelines, Eng. Comput. **37**, 2559 (2020).

19 W. Sun, Z. Yang, and G. Chen, Structural eigenvalue analysis under the constraint of a fuzzy convex set model, Acta Mech. Sin. **34**, 653 (2018).

20 S. Chaube, and S. B. Singh, Fuzzy reliability theory based on membership function, Int. J. Math. Eng. Manag. Sci. **1**, 34 (2016).

21 Y. Ben-Haim, Convex models of uncertainty in radial pulse buckling of shells, J. Appl. Mech. **60**, 683 (1993).

22 I. Elishakoff, P. Elisseeff, and S. A. L. Glegg, Nonprobabilistic, convex-theoretic modeling of scatter in material properties, AIAA J. **32**, 843 (1994).

23 Y. Ben-Haim, A non-probabilistic concept of reliability, Struct. Saf. **14**, 227 (1994).

24 Z. P. Qiu, P. C. Mueller, and A. Frommer, The new nonprobabilistic criterion of failure for dynamical systems based on convex models, Math. Comput. Model. **40**, 201 (2004).

25 Y. W. Zhang, G. Q. Jiang, and B. Fang, RETRACTED: Suppression of panel flutter of near-space aircraft based on non-probabilistic reliability theory, Adv. Mech. Eng. **8**, 168781401663880 (2016).

26 X. Bai, and B. Tu, Ellipsoid non-probabilistic reliability analysis of the crack growth fatigue of a new titanium alloy used in deep-sea manned cabin, Theor. Appl. Fract. Mech. **115**, 103041 (2021).

27 L. Wang, Y. Liu, D. Liu, and Z. Wu, A novel dynamic reliability-based topology optimization (DRBTO) framework for continuum structures via interval-process collocation and the first-passage theories, Comput. Methods Appl. Mech. Eng. **386**, 114107 (2021).

28 R. Wang, X. Wang, L. Wang, and X. Chen, Efficient computational

method for the non-probabilistic reliability of linear structural systems, Acta Mech. Solid Sin. **29**, 284 (2016).

29 S. X. Guo, and Z. Z. Lv, Comparison between the non-probabilistic and probabilistic reliability methods for uncertain structure design (in Chinese), Chin. J. Appl. Mech. **20**, 107 (2003).

30 S. X. Guo, Z. Z. Lv, and Y. S. Feng, A non-probabilistic model of structural reliability based on interval analysis (in Chinese), Chin. J. Comput. Mech. **18**, 5 (2001).

31 S. X. Guo, and Z. Z. Lv, A procedure of the analysis of non-probabilistic reliability of structural systems (in Chinese), Chin. J. Comput. Mech. **19**, 332 (2002).

32 C. Jiang, X. Han, G. Y. Lu, J. Liu, Z. Zhang, and Y. C. Bai, Correlation analysis of non-probabilistic convex model and corresponding structural reliability technique, Comput. Methods Appl. Mech. Eng. **200**, 2528 (2011).

33 C. Jiang, R. G. Bi, G. Y. Lu, and X. Han, Structural reliability analysis using non-probabilistic convex model, Comput. Methods Appl. Mech. Eng. **254**, 83 (2013).

34 H. J. Cao, B. Y. Duan, An approach on the non-probabilistic reliability of structures based on uncertainty convex models (in Chinese), Chin. J. Comput. Mech. **22**, 546 (2005).

35 X. Guo, W. Bai, and W. Zhang, Confidence extremal structural response analysis of truss structures under static load uncertainty via SDP relaxation, Comput. Struct. **87**, 246 (2009).

36 Y. Luo, Z. Kang, Z. Luo, and A. Li, Continuum topology optimization with non-probabilistic reliability constraints based on multi-ellipsoid convex model, Struct. Multidisc. Optim. **39**, 297 (2009).

37 Z. Qiu, and N. Jiang, An ellipsoidal Newton's iteration method of nonlinear structural systems with uncertain-but-bounded parameters, Comput. Methods Appl. Mech. Eng. **373**, 113501 (2021).

38 C. Jiang, Q. F. Zhang, X. Han, J. Liu, and D. A. Hu, Multidimensional parallelepiped model-a new type of non-probabilistic convex model for structural uncertainty analysis, Int. J. Numer. Meth. Eng. **103**, 31 (2015).

39 C. Jiang, Q. F. Zhang, X. Han, and Y. H. Qian, A non-probabilistic structural reliability analysis method based on a multidimensional parallelepiped convex model, Acta Mech. **225**, 383 (2014).

40 B. Y. Ni, C. Jiang, and Z. L. Huang, Discussions on non-probabilistic convex modelling for uncertain problems, Appl. Math. Model. **59**, 54 (2018).

41 C. Jiang, B. Y. Ni, X. Han, and Y. R. Tao, Non-probabilistic convex model process: A new method of time-variant uncertainty analysis and its application to structural dynamic reliability problems, Comput. Methods Appl. Mech. Eng. **268**, 656 (2014).

42 J. Zhan, Y. Luo, X. Zhang, and Z. Kang, A general assessment index for non-probabilistic reliability of structures with bounded field and parametric uncertainties, Comput. Methods Appl. Mech. Eng. **366**, 113046 (2020).

43 Z. Qiu, H. Wu, I. Elishakoff, and D. Liu, Data-based polyhedron model for optimization of engineering structures involving uncertainties, Data-Centric Eng. **2**, e8 (2021).

44 Q. Wei, and H. Yan, A method of transferring polyhedron between the intersection-form and the sum-form, Comput. Math. Appl. **41**, 1327 (2001).

45 C. B. Barber, D. P. Dobkin, and H. Huhdanpaa, The quickhull algorithm for convex hulls, ACM Trans. Math. Softw. **22**, 469 (1996).

46 B. Bueler, A. Enge, and K. Fukuda, Exact volume computation for polytopes: A practical study, Polytopes-Combinatorics Comput. **29**, 13 (2000).

47 R. Rackwitz, and B. Flessler, Structural reliability under combined random load sequences, Comput. Struct. **9**, 489 (1978).

48 T. V. Santosh, R. K. Saraf, A. K. Ghosh, and H. S. Kushwaha, Optimum step length selection rule in modified HL-RF method for structural reliability, Int. J. Pressure Vessels Piping **83**, 742 (2006).

49 Z. Qiu, and J. Wang, The interval estimation of reliability for probabilistic and non-probabilistic hybrid structural system, Eng. Failure Anal. **17**, 1142 (2010).

50 H. Liu, and N. C. Xiao, An efficient method for calculating system non-probabilistic reliability index, Eksploatacja i Niezawodnosc **23**, 498 (2021).

用于具有多失效模式和带相关不确定性结构可靠性分析的基于有限数据的非概率凸多面体模型

邱志平, 唐海峻, 祝博

摘要 本文提出了一种新的非概率可靠性模型, 关注不确定性条件下结构可靠性评估, 称为凸多面体可靠性模型. 与现有的概率和非概率区间模型不同, 凸多面体模型考虑用多维凸多面体描述不确定变量空间. 与区间模型相比, 凸多面体模型更紧凑, 反映了基于有限信息的不确定变量之间的相关性. 在所提出的准则中, 面积/体积比被视作可靠性指标. 然后, 利用基于最可能失效点的线性化方法和分段线性化方法对非线性极限状态函数的情况进行了讨论和处理. 在此基础上, 研究了基于非概率凸多面体可靠性模型的多失效模式结构系统可靠性分析的有效方法. 最后, 通过三个实例验证了该方法的有效性和适用性. 通过与现有可靠性模型的比较, 结果表明, 概率可靠性模型和非概率可靠性模型评估的可靠性是相容的.